Modeling of Multiple Liner Containment Systems for High Speed Rotors

By:

K.A. Dulaney
J.H. Beno
R.C. Thompson

9th EML Symposium, Edinburgh, Scotland, May 1998

PR - 255

Center for Electromechanics
The University of Texas at Austin
PRC, Mail Code R7000
Austin, TX 78712
(512) 471-4496

May 1, 1998

Modeling of Multiple Liner Containment Systems for High Speed Rotors

K.A. Dulaney, J.H. Beno, and R.C. Thompson

The Center for Electromechanics, The University of Texas at Austin

Abstract–**High speed composite rotors typically require containment structures to protect personnel and equipment from high energy rotor material and fragments that result from rotor burst events, which may occur during rotor overspeed. Loading to the containment structure during a burst event is a function of rotor design and containment geometry. A containment system proposed by The University of Texas at Austin Center for Electromechanics uses graphite-reinforced composite cylinders to dissipate radial kinetic energy from the rotor debris and reduce torque loads transmitted to the rotor housing and mounting hardware. Using an analogous mass-spring-damper system, a model was developed with bond graph techniques to estimate containment loads and response. The bond graphs, state equations, and simulation results are compared with experimental results. The model is able to predict the general trends observed in experimental data and is used as a design tool for containment systems.**

Introduction

High speed rotating machines such as composite flywheel energy storage systems may require safety devices to limit collateral damage during rotor bursts (i.e., rapid failure and disintegration of substantial portions of a rotating flywheel that occurs when centrifugal forces generate stresses in excess of the rotor material ultimate stress). Such a failure may occur during an overspeed or may be caused by manufacturing defects. This paper describes a containment system designed by The University of Texas at Austin Center for Electromechanics (UT-CEM) for high speed composite flywheels and the simulation model used in the design process.

Containment Loading

A burst event releases portions of the composite rotor that impact the containment structure at high velocity. Burst events result in three loads to the containment structure: radial, axial, and torsional. Radial loads from contact between the rotor debris and the containment structure are, on average, symmetric about the axis of rotation. However, experimental data suggests that the initial impact is asymmetric in nature resulting in localized high peak loads. Axial loads to the containment structure (i.e., on the end plates) result from the redirection of the radial energy of the debris after impact with the shroud (Fig. 1). Torque loads on the containment mounts (between the containment housing and a vehicle platform, for example) occur because friction between the containment walls and rotating flywheel debris produces a mutual torque between the containment and debris (Fig. 2).

The radial load magnitude depends upon the normal velocity of the flywheel debris relative to the containment wall.

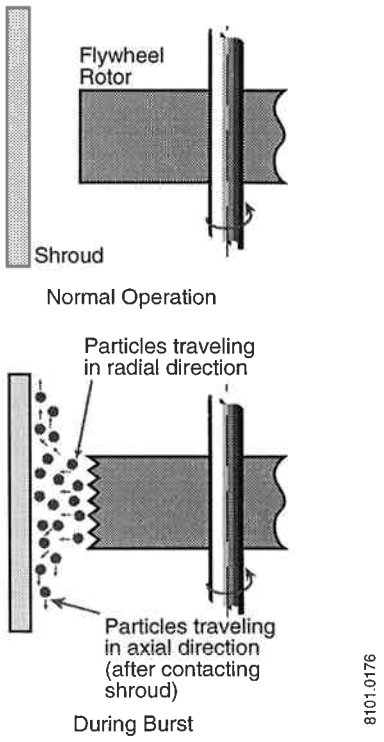

Fig. 1. Axial containment loads result from particle radial velocity being redirected axially after impact with containment liner (much like a water stream is redirected after impacting a wall).

Manuscript received May 1, 1998.

This research was sponsored by UT-CEM and funded by the Defense Advanced Research Projects Agency (DARPA), the Houston Metropolitan Transit Authority, and the State of Texas.

The normal velocity can be calculated from the radial position of the pre-burst rotor particle, a, the inner radius of the containment structure, b, and the angular velocity of the rotor, ω, using the following equation:

$$V_n = a \cdot \omega \cdot \cos\theta \tag{1}$$

where

$$\theta = \sin^{-1}\left(\frac{a}{b}\right)$$

The normal velocity and radial loads experienced by the containment decrease as clearance between the flywheel and the containment structure (b-a) decreases.

Multiple Liner Design

UT-CEM is developing a containment concept that seeks to minimize radial and torque loads resulting from a rotor burst. The containment system uses a rotatable liner inside the rotor housing or shroud. The graphite reinforced composite liner seeks to contain and dissipate the radial energy of the debris and dissipate debris rotational energy through friction. Ideally, the liner has high strength to resist the initial impact and exhibits a low moment of inertia so that the torque produced through friction with the swirling debris tends to rapidly increase the angular velocity of the liner until the liner and debris achieve the same angular velocity. This rapid liner "spin-up" minimizes the heat absorbed by the liner during the transfer of kinetic energy from the debris to the liner. Additional liners of larger diameters could be added to the containment system to provide additional load bearing capability to the first liner (Fig. 3).

Model Development

The multiple liner containment design may be modeled by an analogous mass-spring-damper system. Radial force between flywheel debris and inside liner may be approximated by damped elastic behavior. Collisions between liners can be similarly modeled. Dampers represent dissipation of energy lost during inelastic collisions and due to friction. Fig. 4 shows the diagram for a two liner configuration.

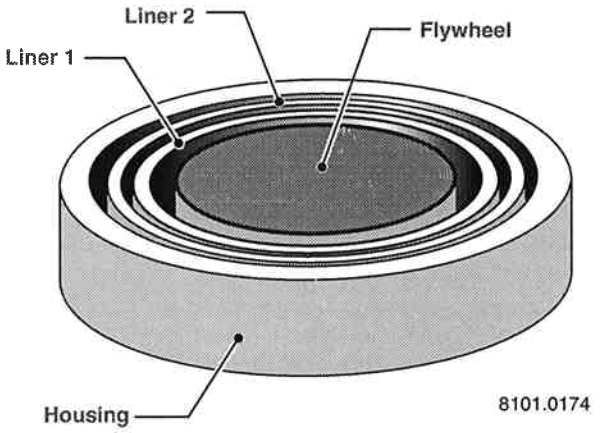

Fig. 3. Containment system consisting of two composite liners inside the exterior (vacuum housing).

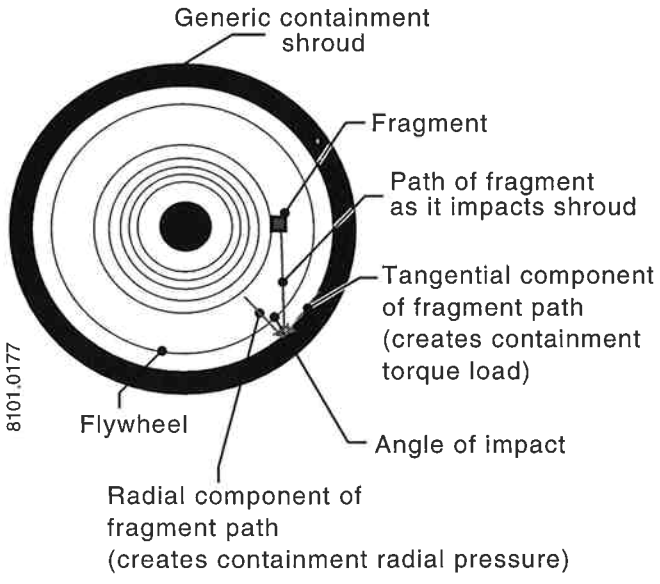

Fig. 2. Radial and tangential containment loads result from the initial particle velocity as flywheel debris breaks away from the flywheel.

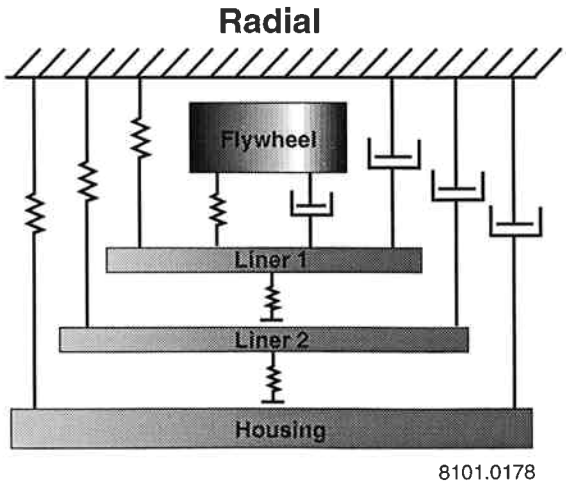

Fig. 4. Schematic for two liner containment system shows basis for modeling radial containment loads.

After a flywheel burst, each liner is modeled as an expanding ring subjected to internal pressure loading, centrifugal force, and, possibly, an external pressure. Reaction (normal) forces exerted by liners are modeled as springs and the energy lost during expansion and contraction of the liners due to material hysteresis are approximated as dampers. From the analogous system diagram, a bond (a systematic method for developing sets of equations that describe complex physical phenomena) graph may be developed in accordance with techniques presented in Beaman and Paynter [1]. A similar diagram was developed to account for rotational motion of the liners, where torque between liners due to frictional contact was represented as a damper. The resulting two bond graphs were combined to account for the relations between the two domains (i.e., radial translation and rotation). The final bond graph is shown in Fig. 5. Although a discussion of bond graph techniques is beyond the scope of this paper, these bond graphs are presented for completeness for the interested reader.

The power input to the bond graph represents centrifugal force acting on flywheel debris. This force varies with angular velocity and so is modulated from the rotational branch of the bond graph. Likewise, friction between rotating liners varies with the normal force that is derived from the radial branch of the bond graph.

The dynamic coefficient of friction between flywheel debris and the first liner is unknown. The high rotational speed of the pre-burst rotor typically results in an initial relative sliding velocity between the debris and the first liner of 500 to 900 m/s. Previous studies have indicated that coefficients of friction at such high velocities vary nonlinearly with the sliding speed [2,3]. Therefore, the model developed from the bond graph calculates the coefficient of friction as a function of sliding velocity.

Constitutive laws for springs which represent radial expansion of the liners were derived directly from equations for the stresses in cylindrical structures due to internal pressures. Equations for stress and strain of cylindrical structures using isotropic material properties are presented in Juvinall [4]. These basic equations were modified to account for orthotropic material properties as seen in composites by substituting appropriate values into the compliance tensor.

First order, ordinary differential equations can be derived from the bond graph and integrated, using standard numerical techniques, to produce the states of the system as functions of time. These states can then be used to plot internal pressure of the inner liner, hoop stress and strain of the inner liner, and torque produced on the shroud, all as functions of time. State equations for this bond graph model are presented here. The states are linear momenta, radial positions, and angular momenta of the flywheel debris, the liners, and the shroud. The angular position of the shroud is also a state of the system. The subscripts *f, 1, 2,* and *s* refer to the flywheel, liner 1, liner 2, and the shroud, respectively. The subscript *g* refers to

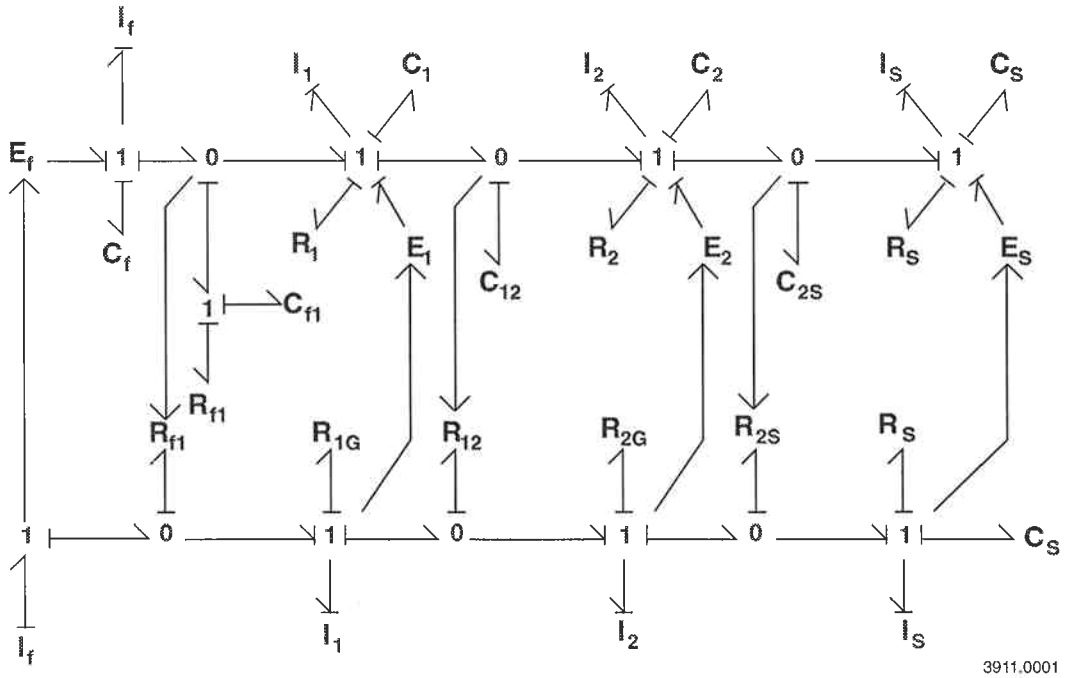

Fig. 5. For completeness, this bond graph is presented. This was used to develop simulation equations for the multiple liner containment system.

rotational ground. Equations (2) through (12) represent radial motion and equations (13) through (17) represent angular motion. Some terms in equations (13) through (17) contain an additional subscript, *a,* to differentiate the angular coefficient from the radial term.

$$\dot{p}_f = m_f r_f \omega_f^2 - k_f x_f - \left[k_{f1} x_{f1} + b_{f1} \left(\frac{p_f}{m_f} - \frac{p_1}{m_1} \right) \right] \quad (2)$$

$$\dot{x}_f = \frac{p_f}{m_f} \quad (3)$$

$$\dot{x}_{f1} = \frac{p_f}{m_f} - \frac{p_1}{m_1} \quad (4)$$

$$\dot{p}_1 = \left[k_{f1} x_{f1} + b_{f1} \left(\frac{p_f}{m_f} - \frac{p_1}{m_1} \right) \right] - \frac{b_1}{m_1} p_1 - k_1 x_1 + m_1 r_1 \omega_1^2 - k_{12} x_{12} \quad (5)$$

$$\dot{x}_1 = \frac{p_1}{m_1} \quad (6)$$

$$\dot{x}_{12} = \frac{p_1}{m_1} - \frac{p_2}{m_2} \quad (7)$$

$$\dot{p}_2 = k_{12} x_{12} - \frac{b_2}{m_2} p_2 - k_2 x_2 + m_2 r_2 \omega_2^2 - k_{2s} x_{2s} \quad (8)$$

$$\dot{x}_2 = \frac{p_2}{m_2} \quad (9)$$

$$\dot{x}_{2s} = \frac{p_2}{m_2} - \frac{p_s}{m_s} \quad (10)$$

$$\dot{p}_s = k_{2s} x_{2s} - \frac{b_s}{m_s} p_s - k_s x_s + m_s r_s \omega_s^2 \quad (11)$$

$$\dot{x}_s = \frac{p_s}{m_s} \quad (12)$$

$$\dot{L}_f = b_{f1a} \left(\frac{L_f}{I_f} - \frac{L_1}{I_1} \right) \quad (13)$$

$$\dot{L}_f = b_{f1a} \left(\frac{L_f}{I_f} - \frac{L_1}{I_1} \right) - b_{1g} \frac{L_1}{I_1} - b_{12a} \left(\frac{L_1}{I_1} - \frac{L_2}{I_2} \right) \quad (14)$$

$$\dot{L}_2 = b_{12a} \left(\frac{L_1}{I_1} - \frac{L_2}{I_2} \right) - b_{2g} \frac{L_2}{I_2} - b_{2sa} \left(\frac{L_2}{I_2} - \frac{L_s}{I_s} \right) \quad (15)$$

$$\dot{L}_s = b_{2sa} \left(\frac{L_2}{I_2} - \frac{L_s}{I_s} \right) - b_{sa} \frac{L_s}{I_s} - k_{sa} \theta \quad (16)$$

$$\dot{\Theta} = \frac{L_s}{I_s} \quad (17)$$

Initial conditions for this system of equations are radial momentum of flywheel debris, p_f (see Equation 1 for calculation of the initial normal velocity), and angular momentum of flywheel debris as it contacts the first liner, L_f.

Experimental Data

With funding from the Defense Advanced Research Projects Agency (DARPA), UT-CEM conducted experiments to determine the radial, axial, and torque loads resulting from a flywheel burst event. A robust steel Instrumented Measurement Device (IMD) was designed and fabricated for an experiment to measure loads on a containment system resulting from a flywheel burst. The IMD was instrumented with strain gages, accelerometers, and a calibrated torque measurement system. Fig. 6 shows the IMD with a test flywheel. The test flywheel was designed with a weak outer "burst ring" so that energy release can be controlled. For the burst event, the flywheel is spun to overspeed via the quill shaft, driven by an air-turbine.

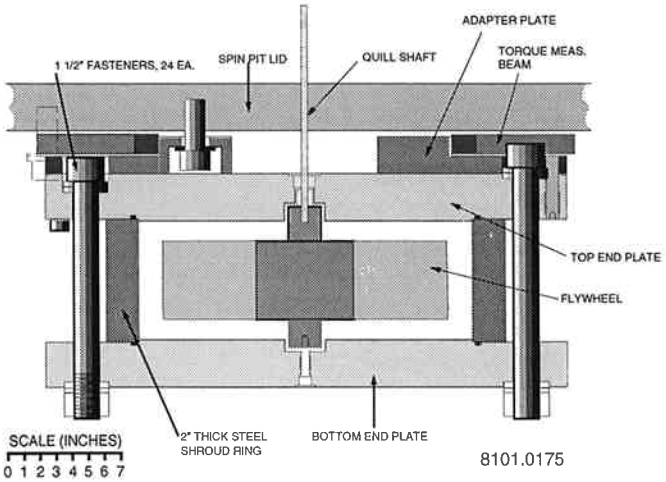

Fig. 6. This diagram depicts the UT-CEM measurement device, which was instrumented with strain gages and accelerometers, to estimate loads that result from flywheel bursts.

A successful test of the IMD (without containment liners) was conducted on February 25, 1997 at Test Devices, Inc. in Hudson, MA. The burst event occurred at 35,350 rpm and released 0.3 kW-hr (1.1 MJ) of energy to the IMD. The most valuable data collected during this test was from the hoop strain gages mounted on the shroud ring and from the torque measurement system. This data indicated an initial impact duration of 70 μs and a peak torque of over 400,000 ft-lb (540,000 N-m).

The hoop strain gage data showed two distinct regions (Fig. 7). Strains in the first region are widely scattered and indicate several oscillations of the shroud, representing initial debris impact and subsequent vibrations. Strains in the second region were much smoother and showed a gradual decrease over time. This indicates a decreasing internal pressure on the shroud as the angular velocity (and radial acceleration) of the flywheel debris decreases due to friction. The torque measurement system data indicated an initial torque spike and then a series of oscillations at a much lower frequency.

Model output closely matches general trends of the data. Predicted hoop strains show both regions described above (Fig. 8). The modeled hoop strain output shows discreet pulses that represent internal pressure variations whereas the measured data shows the general vibrations of the strain gage after the impact event. Modeled torque also shows low frequency oscillations (Fig. 9) that validate the simplified representation of the IMD mount as a torsional spring. However, model parameters could not be adjusted to closely match the peak measured values. This discrepancy may be due to shock and high strain rate effects within the shroud material, which are not accounted for in the model.

As a preliminary trial of the UT-CEM composite liner ring concept, a second burst test within the IMD was conducted on August 7, 1997 at the Test Devices, Inc. facility. For this test, a composite liner of 0.69 in. (0.175 m) radial thickness was placed inside the IMD. The test objective was rapid, inexpensive concept exploration. Consequently, an available composite ring was used as the liner although it was not expected to be adequate for containing the burst. The dynamic radial clearance between the flywheel and liner averaged 0.20 in. (5 mm). The burst event occurred at 45,225 rpm. The liner did not survive the event but the measured hoop strains and torque data were dramatically reduced from the previous test. Post-failure observations indicate that the liner failure likely occurred when the flywheel ring initially impacted the liner, creating an asymmetrical short duration transient peak load. However, this test successfully demonstrated that a rotatable, lightweight, composite liner offers a major benefit as part of a containment system. Table 1 presents a comparison of peak values from test data, indicating an order of magnitude redirection in strain gage readings.

Although the model is unable to account for strains and torques measured after a liner failure, the model did confirm the induced stress levels which led to stress-induced failure of the liner.

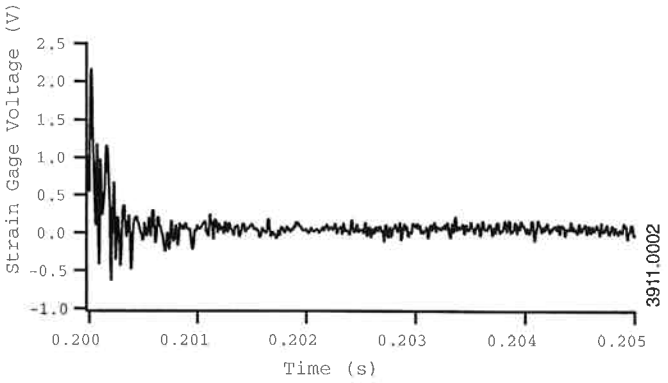

Fig. 7. Sample hoop strain gage measurement, taken from the instrumented measurement device shown in Fig. 6.

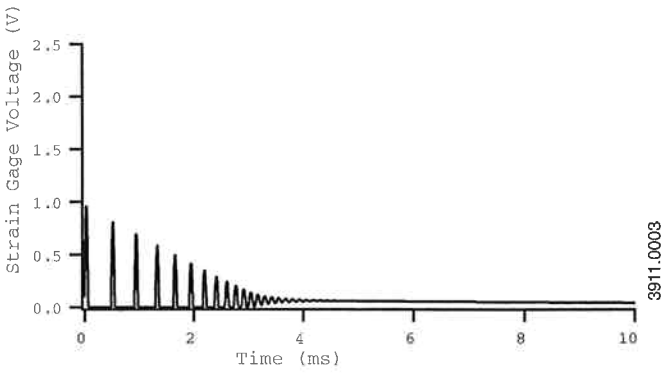

Fig. 8. Hoop strains oscillations as predicted from simulation.

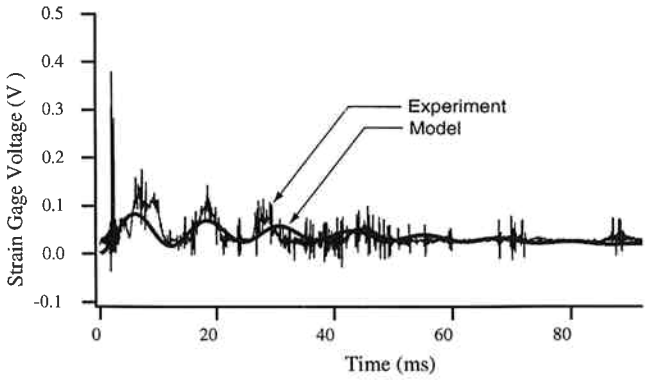

Fig. 9. Comparison of modeled and experimental data. Model does not include mechanisms to capture initial voltage spike, which may be associated with the instrumentation more than physical phenomena.

Table 1. Comparison of peak values from test data

	No Liner	Liner
Burst Speed (rpm)	35,350	45,225
Shroud Ring Hoop Strain (microstrain)	23,000	2300
Bolt Axial Strain (microstrain)	25,000	2200
Torque Beam Strain (microstrain)	10,000	1500

Conclusions

Using data from experimental tests and the bond graph derived model, UT-CEM has developed a design procedure for multiple liner systems to contain rotor debris from a high speed composite rotor burst and verified benefits associated with a containment concept that uses one or more rotatable composite liners.

Research conducted for this paper was sponsored by UT-CEM and funded by the Defense Advanced Research Projects Agency (DARPA), the Houston Metropolitan Transit Authority, and the State of Texas.

Bibliography

1. Joseph J. Beaman and Henry M. Paynter, *Modeling of Physical Systems*, Copyright J. J. Beaman and H. M. Paynter, 1993.
2. F. P. Bowden and D. Tabor, *Friction and Lubrication of Solids, Part II,* pp 472-478, Oxford University Press, 1964.
3. R. C. Zowarka and W. F. Weldon, "Application of a friction model to electromagnetic launchers," 37th Meeting of Aeroballistic Range Association, Courcelette, Quebec, 1986.
4. Robert C. Juvinal, *Engineering Considerations of Stress, Strain, and Strength,* pp 112-128, McGraw Hill Book Company, 1967.